analytical chemistry

Article

pubs.acs.org/ac

Quantum Dots-Based Immunofluorescent Microfluidic Chip for the Analysis of Glycan Expression at Single-Cells

Jun-Tao Cao, Zi-Xuan Chen, Xiao-Yao Hao, Peng-Hui Zhang, and Jun-Jie Zhu*

State Key Laboratory of Analytical Chemistry for Life Science, School of Chemistry and Chemical Engineering, Nanjing University, Nanjing 210093, P.R. China

ABSTRACT: Rich high-quality single-cell information from rare cell sample is very important for the quantitative systems biology description of cellular function. However, this type of data is often prohibited by the conventional analytical technology such as flow cytometry. In this paper, we described a microfluidic platform coupled with a quantum dots-based (QDs) immunofluorescence (IF) approach to measure the expression of glycans on the cell surface of single cells or cell population. Compared with conventional IF staining, the QDs-based IF probe exhibited higher brightness and stability against photobleaching. With the merits of the novel IF staining protocol and microfluidic platform, high-throughput IF staining was performed to measure the glycan expressions and the changes at single K562 cells after drug treatment. The protocol proposed here showed a high sensitivity on the glycan expression profile owing to the amplification of the signal in indirect IF staining. The size of cell sample was only 4×10^3 cells, which made the rare cell sample analysis accessible. This method may find widespread application for assessing cell-surface glycoprotein expression as well as analysis of the heterogeneity in cell populations in a high-throughput manner.

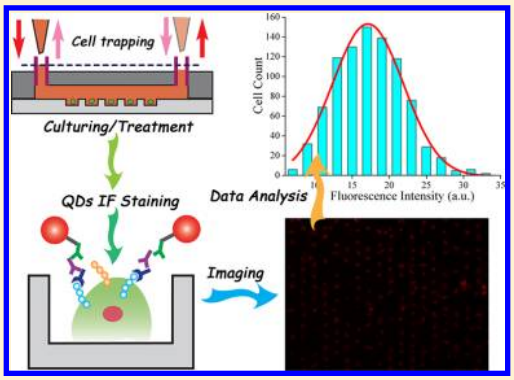

Knowledgement on the behavior of an individual cell is of critical importance because even genetically identical cells showed large variation in gene expression and behavior.[1,2] Flow cytometry (FC) is one of the most common techniques to perform high-throughput single cell data collection, while its capacity to sample rare cell samples was limited. Some other methods, such as optical tweezers, dielectrophoresis (DEP), or acoustic wave, allow efficient trapping and manipulation of single cells for analysis. However, these methods are low-throughput and not yet suitable for cell biological laboratories. To obtain single cell data in rare cell samples in a high-throughput manner facilely, new techniques are needed. One such technique, which has opened up for single cell analysis with more facile cell manipulation, precise reagent introduction, and low reagent consumption, is microfluidics.[3−6] Recently, various microfluidic based arrays have been developed for the single cell analysis.[7−10] Wlodkowic et al. developed a microfluidic platform comprising of an array of micro-mechanical traps to kinetically analyze anticancer agents on hematopoietic cancer cells, which provided new opportunities for automated microarray cytometry and higher-throughput screening.[8] Figueroa et al. reported a method to detect and analyze odorant responses of about 2900 olfactory sensory neurons (OSNs) simultaneously using a microfluidic micro-wells array.[9] These microfluidic microwell arrays validated many systems biology models on patient-derived cells using simultaneous analysis of a large population of cells, whereby the position of individual cells was encoded and spatially maintained over extended periods of time.

Immunofluorescence (IF), as a common laboratory technique, has been widely used both in research and clinical diagnostics. The applications included the evaluation of tissue, cultured cells, or individual cells for the detection of specific proteins,[11,12] small biological molecules,[13] glycans,[14] and so on. In IF techniques, the fluorescent labeled antibodies bound (directly or indirectly) to the target which allowed the detection using wide-field fluorescence or confocal microscopes. The fluorescence difference or variation was always related with abnormal expression of various diseases,[15−17] such as a glycan-related process.[18,19] Cell surface glycans, a large group of biomolecules with diverse structures, presents the upstream information about the cell to the outside world. More evidence indicates that the carbohydrates coated on the cell surface are intimately involved in cell adhesion, differentiation, and immunological recognizations.[20,21] Dynamic changes in the glycan expression have been observed in tumor cell metastasis and cell differentiation.[22,23] Previous techniques established for glycan detection include mass spectrometry,[24] chromatography,[25] and nuclear magnetic resonance.[26] While every strategy possesses distinct advantages, each also suffers its own drawbacks such as lethal destructivity associated with the methodologies, the necessity of laborious procedures, or high cost. To address this, some innovative analysis formats based on ingenious signaling mechanism has been proposed recently.[27−31] For example, Han et al. proposed a fluorescent

Received: September 9, 2012
Accepted: October 19, 2012
Published: October 19, 2012

analysis of dynamic glycan expression using glyconanoparticles and functionalized QDs, which could realize double signal amplification.[27] Zhao et al. reported a robust and specific photoelectrochemical approach for glycan based on a unique biosensing interface consisting of free-base-porphyrin bridged 3-aminophenylboronic acid and titania.[28] In our earlier work, we have developed a microfluidic platform to evaluate the multiglycan expressions on living cells using electrochemical impedance spectroscopy and optical microscopy.[29] The image-based method used therein shows great promise, such as the fast determination process and the facile image analysis, offering an elegant route for understanding the role of glycan in disease development as well as to help guide treatments.

In conventional IF assay, the organic dyes or fluorescent proteins were labeled with the antibody that recognized the antigen of interest directly or indirectly. As with most fluorescence techniques, a significantly problem with IF was photobleaching. Quantum dots (QDs), the new semiconductor nanocrystals, with higher brightness and stability against photobleaching,[32,33] have achieved encouraging developments in cellular and in vivo molecular imaging, especially in the cancer research field.[27,34,35] QDs based fluorescent probes have been developed for glycan expression analysis.[36−38] In these methods, the QDs were directly functionalized with molecules such as phenylboronic acid or lectins to specifically recognize the sugar epitope on the cell surface. Pang et. al developed a QDs-based IF technology for the quantitative, sensitive, and accurate determination of HER2 in breast tissue.[39] In our previous report, QDs had been used to probe the apoptotic cells in a microfluidic device for drug screening, which bridge the gap between the QDs based in vitro cell imaging and the analysis of individual cell in a microfluidic system.[40]

Herein, we reported a QDs-based IF approach using a microfluidic cell array device to quantify the glycan expressions and the changes on the K562 cells after 2-deoxy-D-glucose (2-DG) treatment. The microfluidic platform comprises an array of microwells allowing passive capture of individual non-adherent and adherent cells in rare cell samples. All the cells on the array were addressable even for a short time culturing, which was difficult in the conventional method, especially for the nonadherent cells. Compared with the organic fluorescence probe used in conventional IF staining, the QDs-based fluorescence probe provides higher brightness and stability against photobleaching.

MATERIALS AND METHODS

Microfluidic Array Fabrication. The microfluidic device was fabricated using PDMS (Sylgard 184, Dow Corning) by the standard soft lithography method.[41] Two negative photoresist SU-8 (Microchem, Newton, CA)-based molds were used to generate the microwells and the microfluidic channels, respectively. The fabrication process followed the previously reported protocols.[42] The schematic diagram of the overall microfluidic device was shown in Figure 1A. Briefly, two photomasks (printed at 10 000 dpi, Meijingwei Photo-electronics Co., Ltd., Suzhou, China), one for the microwells comprised of 1400 wells and one for fluidic layers with microchannels and a culturing chamber, were used to generate our master molds. The molds of the microwell and the fluidic layer with thickness of 25 and 50 μm were fabricated by the SU-8 photoresist, respectively. The fluidic layer was made by pouring PDMS (10:1, elastomer to cross-linker ratio) onto its mold to a thickness of 2 mm and cured in 70 °C for 2 h. Prior to pouring the PDMS onto the mold of the fluidic layer, two tips of silicone tubes were glued onto the surface of the master mold to serve as an inlet and outlet. While the microwell layer of the chip was made by spin-coating PDMS (5:1, elastomer to cross-linker ratio) onto the microwell mold at 500 rpm for 30 s to a thickness of 0.2 mm, and baked for 70 °C for 2 h. The cured layers were peeled from the master carefully. The microwell layer was transferred onto a coverslip. The fluidic layer was irreversibly bonded on the microwell layer to form a

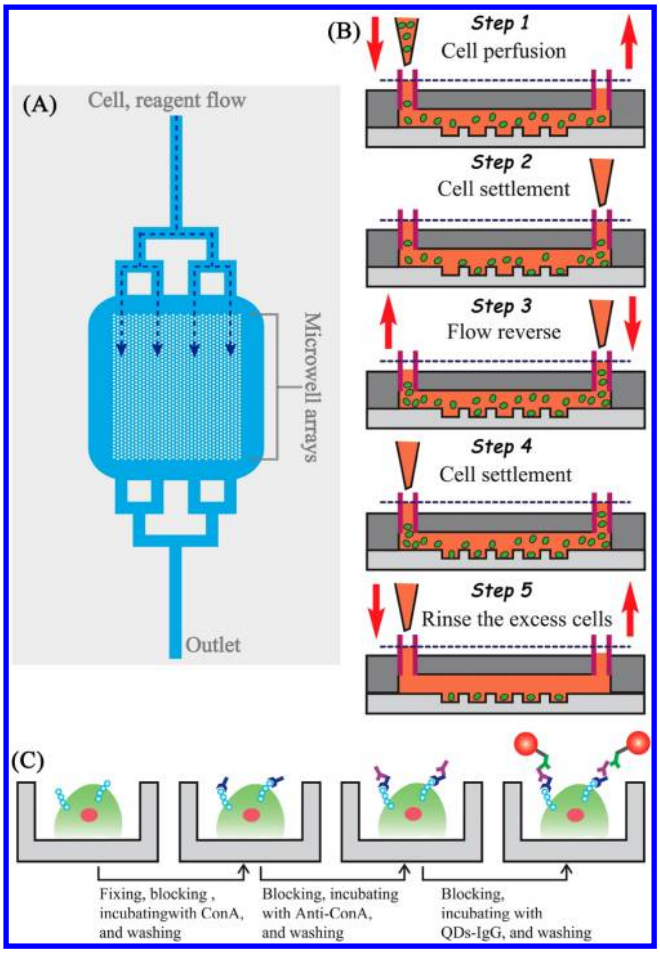

Figure 1. Schematic of a microwell array-based analysis of glycan expression on individual cells in microwells. (A) A schematic diagram of the overall microfluidic device. Branching delivery channels ensured more equal distribution of flow with cells and reagents to each part of the chamber. Only one inlet and outlet were needed, cell and reagent flow were introduced from the upper inlet and entered the microwell arrays by hydro-gravity. (B) The process of cell suspension introducing and single cell trapping. A volume of 2.0 μL of K562 cell suspensions were introduced into the device (step 1). The flow was stopped, and the cells were allowed to settle down into the microwells (step 2). A drop of PBS was introduced into the outlet to reverse the flow direction, and the cells in the outlet were passing through the microwell region again (step 3). The flow was halted to allow the cells to settle down into the microwells (step 4). This process was repeated two or more times to achieve a satisfactory single cell occupancy. Then extra PBS medium immediately introduced into the inlet for removing out the residual cells between the microwells in the microchamber (step 5). (C) Schematic drawing of the microfluidic IF staining process. The major process followed as fixing → blocking → Con A incubating → washing → blocking → anti-Con A antibody incubating → washing → blocking → QDs-IgG incubating → washing and observation.

sealed device using oxygen plasma treatment (Harrick Scientific Corporation, Ossining, NY).

Cell Culture and Treatment. The K562 cell line from Nanjing KeyGen Biotech Co., Ltd. was cultured in RPMI 1640 medium (Gibco, Grand Island, NY) containing 10% fetal calf serum (HyClone, Logan, UT), 100 units mL^{-1} penicillin, and 100 $\mu g\ mL^{-1}$ streptomycin at 37 °C in a humidified incubator containing 5% CO_2. The cells at the logarithmic growth were collected and separated from the medium by centrifugation at 1000 rpm for 6 min and then washed three times with a sterile phosphate buffer saline (PBS, pH 7.4). The supernatant was aspirated, and the cell pellet was resuspended in the PBS to obtain a homogeneous cell suspension. Cell number was determined using a Petroff-Hausser cell counter. 2-DG (Sigma-Aldrich Inc.) treated K562 cells were obtained by incubating the cells in a culture medium containing 20 and 80 mM 2-DG for 12 h, respectively.

Chip Loading and 2-DG Treatment. The microfluidic device was autoclaved before use. To avoid air bubbles trapped in microwells, the device was primed with 75% ethanol (v/v) and vacuumized for 3 min. Following the ethanol treatment, 0.01 M PBS (pH 7.4) was used to rinse the system for 3 min. Then the device was fulfilled with 2% BSA in PBS at 37 °C for 30 min to block the microwell array surface.

The introduction of single cells from cell suspension into microwells was shown in Figure 1B. Initially, 2 μL of the cell suspensions (2.0×10^6 cells mL^{-1}) was introduced from the inlet of the device, which led the cells flow from up to down the microwell arrays by hydro-gravity (Figure 1B, step 1). Subsequently, the inlet and the outlet volume with PBS were counterpoised, and the flow was halted for 3 min to allow the cells to settle down into the microwells (Figure 1B, step 2). Then, a drop of PBS was introduced into the outlet to reverse the flow. The cells in the outlet passed through the microwell region (Figure 1B, step 3) to allow more cells to settle down into the microwells (Figure 1B, step 4). This process was repeated two or more times to achieve a satisfactory single cell occupancy. Finally, the cell samples in the inlet were genteelly aspirated out and an extra 2 μL of PBS medium was immediately introduced into the inlet to remove the residual cells between the microwells in the microchamber (Figure 1B, step 5).

For on chip cell culturing, a reservoir (diameter of 5 mm, height of 5 mm, and total volume of about 100 μL) was equipped gently. A syringe pump (Baoding Longer Precision Pump Co., Ltd.), loaded with a 1 mL syringe at the outlet, pulled the culture medium to generate a flow rate of 50 $\mu L\ h^{-1}$. After 24 h culturing, the cell viability solution containing calcein-AM (Ex/Em = 490 nm/515 nm), and PI (Ex/Em = 535 nm/615 nm) (Dojindo Lab., Kumamoto, Japan) was introduced to stain the cells. To evaluate the glycan expression under drug treatment, the chip was continuously perfused with 2-DG for 12 h. QDs 605-goat antihuman IgG (QDs-IgG, Em = 605 nm, Jiayuan Quantum Dots Corporation, Wuhan, China) were used to probe the glycan variation on the cell surface.

Microfluidic IF Staining. The staining conditions were screened to optimize the concentrations of concanvalin A (Con A, Sigma-Aldrich), primary (anti-Con A antibody, Sigma) and secondary antibodies (QDs-IgG), incubation time spans, and the washing and blocking steps. Under the optimized staining conditions, the QDs based IF staining for the glycan expression was performed. The microfluidic IF staining process was shown in Figure 1C. The 4% w/w paraformaldehyde solution in PBS was added to fix the cells trapped in the microwells for 10 min at 25 °C. After fixation, the cells were rinsed with TBS for 10 min and 2% BSA for 30 min to block the nonspecific binding sites on the cell surface. Con A treated with various concentrations of mannose (0, 0.2, 1.0, 1.5, 3.0 mM) was introduced into the chip and incubated with the cells for 10 min in PBS containing 1 mM Mn^{2+} and 1 mM Ca^{2+} at room temperature to conjugate with the carbohydrate moiety on the cell surface. Afterward, the cells were rinsed with TBS-T containing 0.05% Tween 20. After blocking with 2% BSA for 10 min, anti-Con A antibody was introduced into the device and incubated for 1 h and the washing and blocking steps were performed subsequently. Then the resulted microwell array was treated with QDs-IgG for probing the mannosyl group on the cell surface. In the drug treatment assay, IF staining was carried out after the exposure of the cells to 2-DG for 12 h.

Chip Imaging and Data Analysis. Fluorescence images were acquired using a Nikon TE2000-U inverted fluorescent microscope equipped with a cooled CCD camera (DS-U1, Nikon Corporation, Japan). Fluorescent images were analyzed using the Nikon imaging software NIS Elements (Nikon Corporation, Japan). The average fluorescence intensity of each cell region was corrected by subtracting the average local background fluorescence of the empty wells in the array.

Flow Cytometric Analysis. K562 cells were treated with or without 2-DG (20, 80 mM in culture medium) for 12 h. Then the cells were collected, centrifuged, and washed with sterile cold PBS, respectively. The cells with 2-DG treated were incubated with 15 $\mu g\ mL^{-1}$ Con A-FITC. The K562 cells without 2-DG treated were incubated with 15 $\mu g\ mL^{-1}$ Con A-FITC (blocked with 0, 0.2, 1.0, 1.5, 3.0 mM mannose) for 30 min at room temperature, respectively. The cells were collected by centrifugation, washing with sterile cold PBS, and resuspended in 500 μL of PBS. The sample was immediately analyzed on the flow cytometer (Becton Dickinson) and confocal laser scanning microscopy (CLSM) with excitation at 488 nm.

RESULTS AND DISCUSSION

Cell Loading in the Microwell Array. High single cell occupancies in the microwell arrays are important for the high-throughput analysis. Rettig et al. presented an optimization study to obtain high single-cell occupancies for two cell types in large arrays of microwells.[42] In our system, the microwell size with different diameters of 20, 30, and 40 μm were tested. The microwell depth and interwell distance (edge to edge) were fixed at 25 and 15 μm. As a result, the microwell with a diameter of 20 μm showed an overall cell occupancy of 30%. Almost all the occupied microwells included a single cell. In the case of microwells with 40 μm, the overall occupancy was nearly 100%, while the microwells with two to four cells increased significantly. As for the microwell with a diameter of 30 μm, the overall occupancy was approximately 90%. Compared with the other two sizes, the single cell occupancy increased obviously. In the flow system, the settle procedure was pivotal for the single cell trapping. To simplify the cell trapping for the rare cell sample, a come-and-go flow of the cell suspension in the device was used. The cell suspension flow direction was reversed by adjusting the inlet and outlet volume facilely. This procedure reversed the cell flow and thus created the opportunity for the cells to be settled into the empty microwells. Using this strategy, the limited cells could be

located into the microwells without excess addition of cell suspensions.

To obtain high single cell occupancy, the settle time was also an important parameter. In this system, the settle time was only 3 min after the flow halted, which was shorter than that reported with the microwell arrays.[43] In the microwell arrays, the cell suspension was pipetted onto the array for settling. The cells in the upper of the drop had a relative long travel distance to the microwell array surface, which prolonged the settle time. However, in the microfuidic microwell system, the cell suspension in the cell chamber was limited to tens of micrometers dimension space, which shortened the travel distance of the cells in the suspension to the microwell. The decreased distance shortened the settle time and thus reduced the experiment duration and increased the cell viability. As shown in Figure 2, the single-cell occupancy was ~70% under

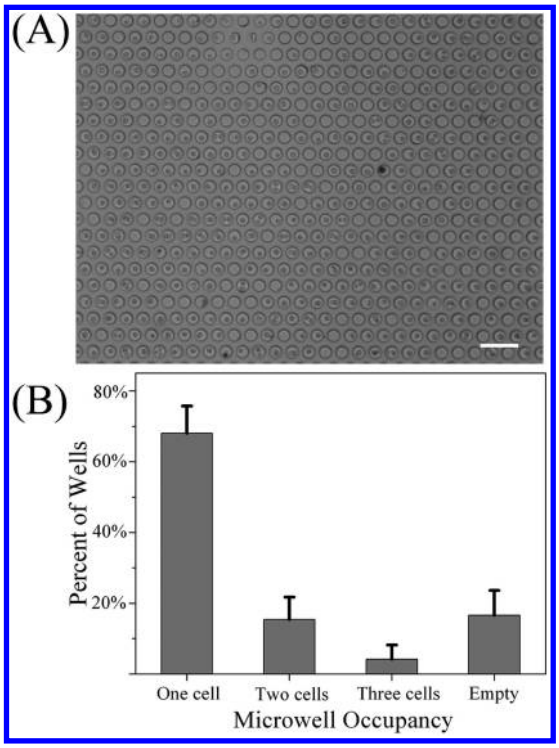

Figure 2. (A) Photo taken after cell trapping. Scale bar, 100 μm. (B) Distribution of microwell occupancies for K562. Each vertical bar depicts the percentage of microwells occupied by a single cell, two cells, three cells, or no cells. There are no more than three cells in the well in this platform. Error bars come from parallel experiments on three chips.

the optimized procedure. A higher occupancy could be achieved by repeating the trapping procedure, whereas the longer duration time may influence the cell viability.

Cell Viability. To characterize the cell viability on the present device, cell viability solution containing Calcein-AM and PI was introduced to stain the cells. The results in Figure 3 showed that almost all the cells trapped in the microwells kept high viability after 24 h culturing. The high viability of cells in microwells were attributed to shorter settle time, relative larger microwell space, and the protection of cells from the shear stresses by laminar flow conditions above the wells.[44] Compared with the presentation just after cell seeding, more microwells with two cells were observed after 24 h culturing.

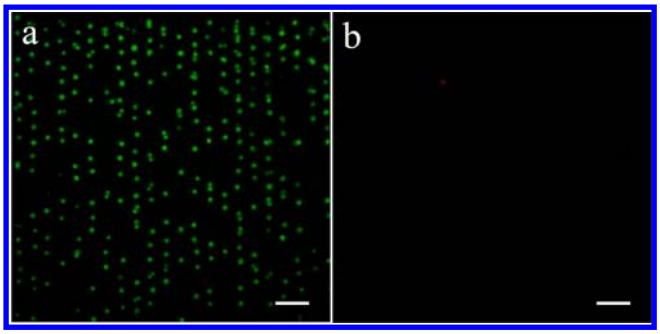

Figure 3. Viability analysis of the cells cultured within the microfluidic arrays. Fluorescence micrographs of K562 cells in microwells labeled with calcein AM (a) and PI (b). Cells were cultured under continuing perfusion of culture medium with a flow rate of 50 μL h^{-1} for 24 h. Scale bars, 100 μm.

The change was ascribed to the proliferation of the single cells in the microwells.

Optimization for IF Staining. In IF analysis, to achieve the high sensitivity and high-resolution in visualization of the target, the concentrations of primary and secondary antibodies, and different incubations time spans in the labeling protocol needed to be optimized. The microfluidic IF staining procedure in this system was shown in Figure 1C. Con A, a lectin of carbohydrate-binding protein, was used to bind to the mannosyl groups on the cell surface by the specific recognization of Con A and the mannosyl group.[45] The initial Con A concentration for recognition was critical for the measurement of the expression extent of carbohydrates on the K562 cell surface. To screen the proper concentration of Con A, the concentration range from 2 to 100 μg mL^{-1} was tested. The results were recorded as the average fluorescence intensity of the individual cells. Figure 4a showed the plot of the average fluorescence intensity vs Con A concentration. The average fluorescence intensity increased to a maximum value at 15 μg mL^{-1}. At the concentration lower than 15 μg mL^{-1}, the Con A might be insufficient for binding on K562 cells. When the concentration was higher than 15 μg mL^{-1}, the steric hindrance among the protein molecules may interfere the Con A binding to the cells.[30] The Con A concentration of 15 μg mL^{-1} achieved a saturated binding of Con A to mannosyl groups on the cell surface.

The recognition time was an important parameter for the kinetic binding between lectins and cell surface carbohydrates. As shown in Figure 4b, the fluorescence intensity increased with the time and tended to a constant value at 10 min, which indicated the sufficient binding of the Con A conjugate to mannosyl groups on the cell surface. Therefore, the effective binding between the Con A and the cell was accomplished within 10 min, which was shorter than 30−60 min required in lectin array-based methods.[23,30] The decreased recognition time demonstrated the fast diffusion process in the present microenvironment.

The anti-Con A was used not only as primary antibody to recognize Con A but also a linker to specifically conjugate with the fluorescence probe, QDs-IgG. The various concentration of anti-Con A was tested. The corresponding concentrations of QDs-IgG were 0.1 μM or 0.05 μM, and the incubation time was 30 or 60 min. As shown in Figure 4c, the anti-Con A concentration higher than 30 μg mL^{-1} did not make any significant improvement. To obtain the optimal incubation time, the time-lapse images after introducing 0.1 μM QDs-IgG

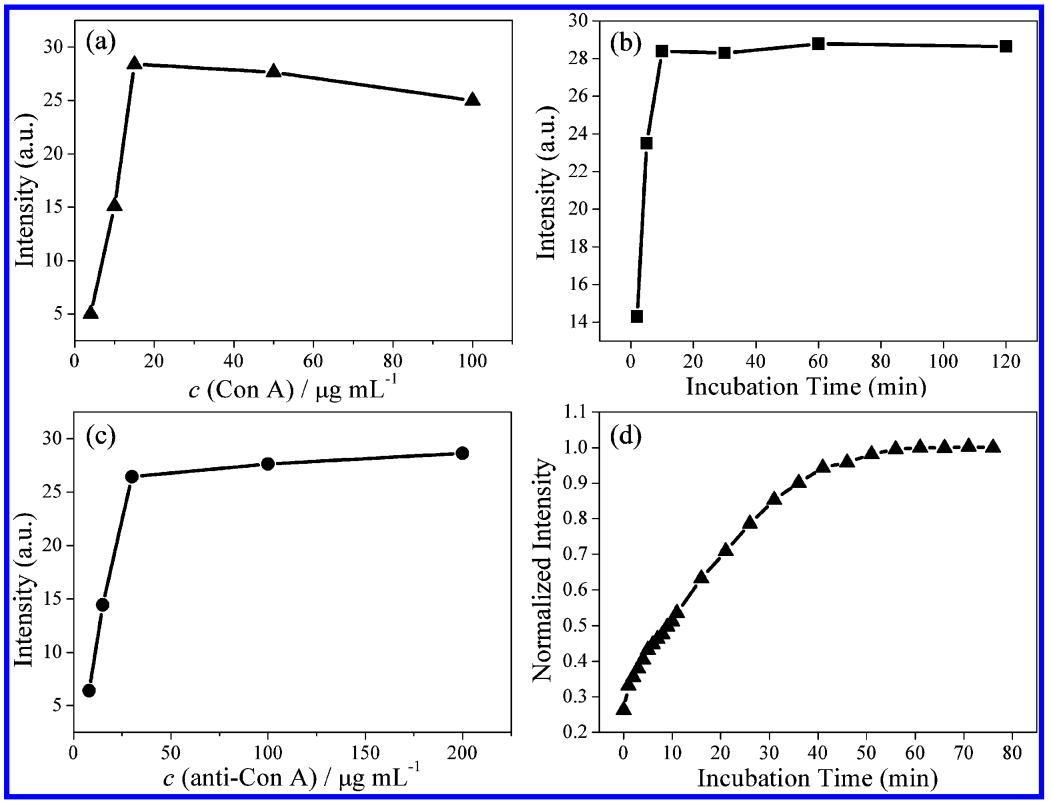

Figure 4. Optimization for the IF staining: (a) average fluorescence intensity at different concentration of Con A, (b) average fluorescence intensity at different incubation time of Con A to the cell surface, (c) average fluorescence intensity at different concentrations of anti-Con A to the cell surface, (d) time-lapse analyzes the intensity variation of the QDs-IgG stained cells at different time points after introducing 0.1 μM QDs-IgG. The fluorescence images were taken with a 20× objective (0.25 s exposure). Fluorescent intensity of individual cell was estimated by Nikon imaging software NIS Elements, and the intensity values were normalized. All other conditions were at the optimum conditions.

were taken. Figure 4d represented the variation of the normalized intensity at different time points after introducing QDs-IgG. When the incubation time increased, the normalized intensity increased and tended to a constant value at 60 min, indicating the sufficient conjugation between the anti-Con A and QDs-IgG. It was noted that the QDs-IgG concentration at 0.05 μM gave faint fluorescence even with longer incubation time, which was too weak to be analyzed. Thus, the optimal condition included 30 μg mL^{-1} anti-Con A and 0.1 μM QDs-IgG with 1 h incubation.

However, some nonspecific background signal was observed under the optimum conditions. The surface of cell and hydrophobic PDMS could nonspecifically adsorb Con A, anti-Con A, and/or QDs-IgG to give background fluorescent signal. To eliminate the nonspecific adsorption, the chip was initially incubated with 2% BSA for 30 min before cell seeding. The blocking solution containing 2% BSA and the washing solution added with 0.05% Tween 20 in TBS were used after each step with protein introduction. The results showed that 15 min for washing solution and 10 min for blocking solution were sufficient to eliminate almost all nonspecific signals to obtain a clear background.

Fluorescent Imaging. With the above-mentioned optimum conditions, the QDs based IF staining was performed to profile the mannosyl groups on the K562 cell surface. The expression level of the mannosyl motifs on the cell surface was correlated with the fluorescence intensity in each individual cell. Figure 5 showed the typical fluorescence images of the QDs-IgG based IF staining for K562, while the red fluorescence of QDs showed uniform dispersion on the cell surface, which indicated the distribution of the mannosyl groups on the cell membrane. All the cells in the occupied wells could be probed with the QDs-IgG sensitively, which exhibited the good performance of the QDs based IF staining in the microfluidic system. Interestingly, there were slight variations in the QDs intensity from well to well. The variations in the fluorescence intensities indicated that the mount of mannose motifs on the individual cell surfaces were different. The heterogeneity of the cells in the glycosylation profile existed even though the population of the genetically engineered cell lines was from a single parental cell.[1] The effective imaging performance of the present IF method was competent for the high-throughput single cell analysis.

Evaluation of Mannosyl Groups on the Cell Surface. Glycosylation is a major form of post-translational modification and the variation in glycosylation is associated with cell differentiation and malignant transformation.[46] The specific carbohydrate−lectin recognition events are being widely employed as a tool for the cell surface glycosylation profiling.[22] To further investigate the performance of the present method on the glycosylation profiling, mannose−Con A was selected as an initial proof-of-concept recognization pair to evaluate the amount of mannosyl groups on the cell surface. In this strategy, the fluorescence signal was directly related to the amount of QDs-IgG conjugated to the anti-Con A−Con A complex on the cell surface. Meanwhile, the Con A conjugated on the cell surface depended on the expression levels of mannosyl groups on each cell surface. Namely, the fluorescence signal on the cell surface reflected the expression of the mannosyl groups on the cell surface. To evaluate the expression of these carbohydrate

dx.doi.org/10.1021/ac302609y | Anal. Chem. 2012, 84, 10097−10104

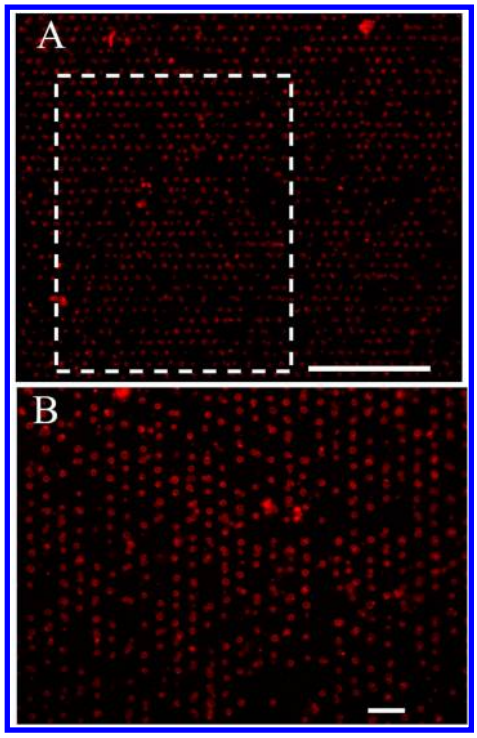

Figure 5. Fluorescence micrograph of QDs-IgG immunofluorescence for K562. (A) Large-area fluorescence microscopy imaging using a 4 × objective with 1.5 × magnification (1 s exposure). Cells were prefixed, treated with Con A, and then stained with anti-Con A and QDs-IgG. Scale bar, 500 μm. (B) The fluorescence image rotated 90° (white dashed box in part A) taken with a 10× objective (0.25 s exposure). Scale bar, 100 μm.

motifs on the cell surface, an experiment was designed by partly blocking the specific binding sites of Con A with mannose solutions at different concentrations for 1 h. The resulting solution was introduced to the cell containing microfluidic microwell array. Because of the partly blocked mannose-specific binding sites, the Con A conjugated to the mannosyl groups on cell surface decreased, resulting in a relative lower fluorescence intensity compared to that obtained without blocking (Figure 6A–C). Fitting each individual cell fluorescence response yielded a histogram of the fluorescence distribution for the Con A treated with mannose at different concentrations (Figure 6D). As can be seen in Figure 6D, with an increase of the mannose concentration, the fluorescence intensity of the cells decreased. It is noted that inhibition efficiency (Δ%) exhibited a linear relation with mannose concentration (Figure 6E). The inhibition efficiency obtained was calculated as follows: $\Delta\% = [1 - (I_b/I_0)] \times 100\%$, where I_b was the fluorescence intensity value obtained with cells treated with Con A blocking with mannose at different concentrations and I_0 is that from cells with Con A without blocking. With the mannose concentration increase, the binding sites of the Con A decreased, thus the fluorescence intensity of individual cell decreased. The mannose concentration used was directly related to the mannosyl group on the cell surface, which could be used to evaluate the glycan expression at single cell levels.

The similar experiment was performed using the FC method as a technique to measure the variation of the fluorescence intensity of cells in response to the partial blocking. As shown in Figure 6E, the similar linear relationship was also obtained with less inhibition efficiency. The difference might be attributed to two reasons. One was that the molecular delivery in microfluidic system was faster than that in bulk solution,

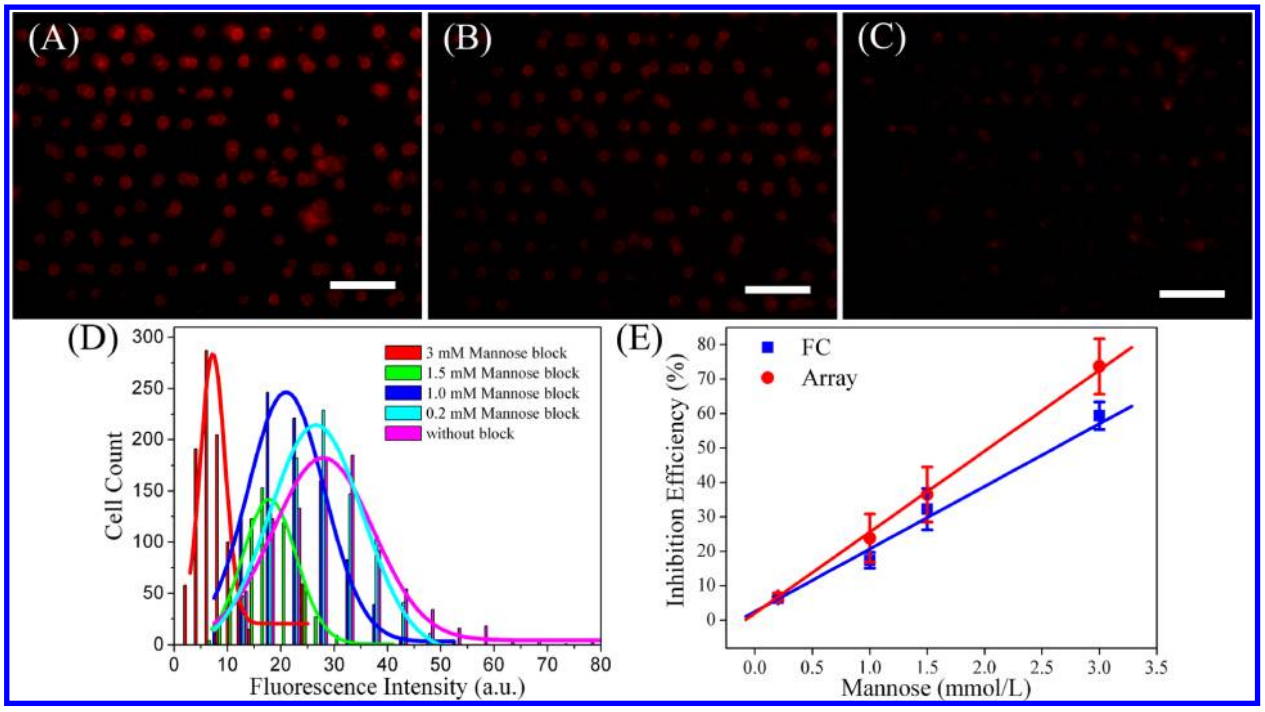

Figure 6. Fluorescence images of cells on a chip treated with Con A without blocking (A), Con A blocking with 1 mM mannose (B), and Con A blocking with 3 mM mannose (C). The fluorescence images were taken with a 20× objective (0.25 s exposure). Scale bars, 100 μm. (D) A histogram of the predicted average fluorescent intensity of single cell after blocking Con A with a different concentration of mannose or not. (E) Effect of the amount of mannose used to block Con A on the decrease of fluorescence intensity was quantified by an array chip and a conventional flow cytometer. Parallel samples were separately analyzed using either a conventional flow cytometer or microfluidic cell array.

dx.doi.org/10.1021/ac302609y | *Anal. Chem.* 2012, 84, 10097–10104

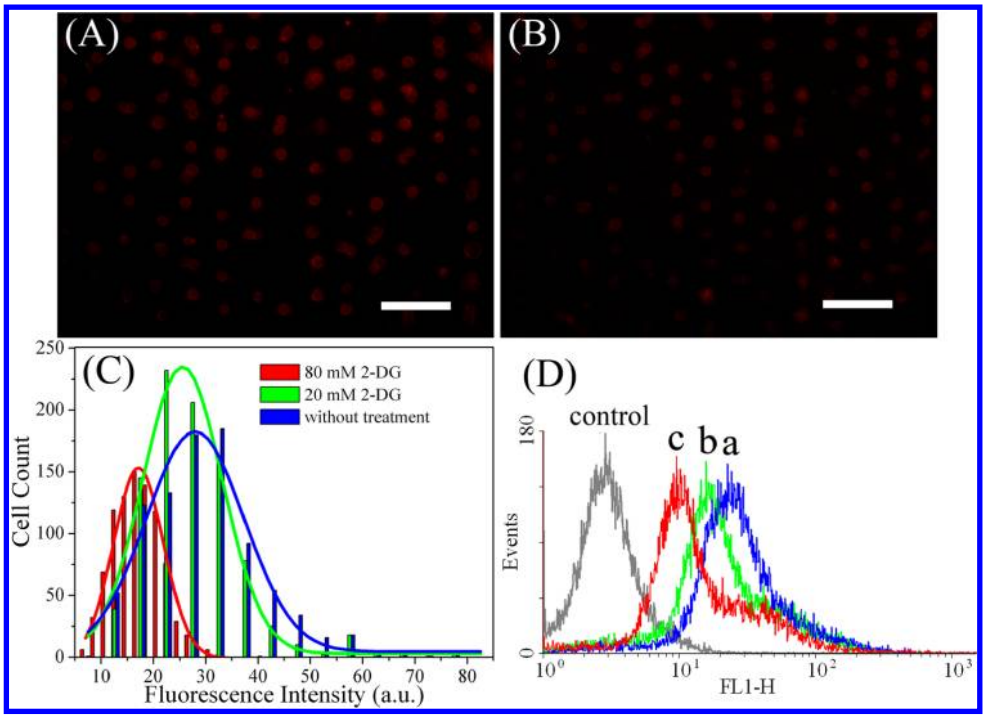

Figure 7. Fluorescence images of cells treated with 20 mM (A) and 80 mM 2-DG (B). The fluorescence images were taken with a 20× objective (0.25 s exposure). Scale bars, 100 μm. (C) A histogram of the predicted average fluorescent intensity of single cell with 2-DG treatment. (D) Fluorescence profile of K562 cells treated with or without 2-DG treatment. K562 cells without treated (a), treated with 20 mM (b) or 80 mM (c) 2-DG were cultured for 12 h, and the appearance of the surface fluorescence was monitored by FC using Con A-FITC.

which means the Con A conjugated more efficiently with the cell in the microfluidic system in a short time (10 min) than that in the bulk system with a longer incubation time (30 min). The other was that the Con A used in the microfluidic system was wild type without any modification, while the Con A in the FC was labeled with FITC. The steric hindrance due to the fluorescence tag can cause different behaviors for Con A.[47]

The microfluidic device can be used to sample a greatly reduced number of cells when compared with FC. The size of cell sample was only 4×10^3 cells. It was noted that this indirect IF staining strategy could be used to obtain more sensitive profiles of glycans with low abundance than that with FITC or QDs-labeled lectins, which was due to amplification of the signal in indirect IF staining because more than one secondary antibody can attach to each primary. Furthermore, we suggested that our technology was likely to become a useful assistant technique to conventional FC in situations where rare cell samples needed to be analyzed or high-throughput single cell information needed.

Evaluation of Glycan Expression on Cells in Response to 2-DG. 2-DG can block glycolysis[48−50] and interfere with asparagine(N)-linked glycosylation of their coated proteins in certain viruses,[51−54] which can be utilized to monitor the dynamic changes of glycans on the cell surface in response to drugs. The effects of 2-DG exposure on pattern expression of glycans on a cell surface were shown in Figure 7. Compared with the untreated cells in Figure 6A, the fluorescence intensity of the cells decreased after 2-DG treatment. The fluorescence decrease reflected a lower amount of mannosyl residues on the cell surface after 2-DG treatment (shown in Figure 7A,B). Fitting each individual cell fluorescence response yielded a histogram of the fluorescence distribution for the cell treated with 2-DG (Figure 7C). The expression of the mannosyl groups on K562 cells showed a decrease of 8.2% and 38.3% for 20 mM and 80 mM 2-DG treatment, respectively. It was noted that the mannosyl groups on the cell surface decreased after the drug treatment, and the decrease exhibited a dose dependent manner. 2-DG was reported to interfere with N-linked glycosylation, which decreased the glycoprotein in the cells.[51,55] However, the distribution of glycoprotein in the membrane after the drug treatment was unknown. Our method presented here provided a direct tool to characterize the glycan residues on the cell surface, which was the final destination of the glycan. The FC analysis of Con A-FITC binding to K562 with or without 2-DG treatment confirmed these findings (Figure 7D).

■ CONCLUSIONS

A microfluidic device integrated with a microwell array has been developed to profile the glycan expression on the cell surface in a high-throughput manner by the IF staining protocol using QDs as the probe. The QDs based indirect IF staining protocol used here was more sensitive than that with the direct FITC or QDs-labeled lectins because of the amplification of the signal in indirect IF staining, which was more suitable for the analysis of glycans with low abundance. Meanwhile, the microfluidic device used allowed the analysis of low cell samples in a high-throughput manner with the ease of operation. By integrating the microfluidic technology, the nanotechnology based IF staining protocol, and specific recognition between bimolecules, high-quality IF images were obtained, in which single cell behavior and the population information could be obtained simultaneously. The strategy was used to evaluate the glycan expression profile and the changes in the glycome under 2-DG treatment effectively and information rich. The availability of this QDs-based IF microfluidic platform provides a significant tool to meet the even more challenging questions in the field of

glycomics and to sensitively analyze glycan heterogeneity on the cell surface.

AUTHOR INFORMATION

Corresponding Author

*Phone/fax: (86)2583597204. E-mail: jjzhu@nju.edu.cn.

Notes

The authors declare no competing financial interest.

ACKNOWLEDGMENTS

This work is supported by National Basic Research Program of China (Grant 2011CB933502) and the National Natural Science Foundation of China (Grants 50972058, 21121091, and 21020102038)

REFERENCES

(1) Sethuraman, N.; Stadheim, T. A *Curr. Opin. Biotechnol.* **2006**, *17*, 341−346.
(2) Rao, C. V.; Wolf, D. M.; Arkin, A. P. *Nature* **2002**, *420*, 231−237.
(3) Kovarik, M. L.; Gach, P. C.; Ornoff, D. M.; Wang, Y.; Balowski, J.; Farrag, L.; Allbritton, N. L. *Anal. Chem.* **2012**, *84*, 516−540.
(4) Zare, R. N.; Kim, S. *Annu. Rev. Biomed. Eng.* **2010**, *12*, 187−201.
(5) Ji, J.; Zhao, Y.; Guo, L.; Liu, B.; Ji, C.; Yang, P. *Lab Chip* **2012**, *12*, 1373−1377.
(6) Li, L. M.; Wang, W.; Zhang, S. H.; Chen, S. J.; Guo, S. S.; Français, O.; Cheng, J. K.; Huang, W. H. *Anal. Chem.* **2011**, *83*, 9524−9530.
(7) Carlo, D. D.; Aghdam, N.; Lee, L. P. *Anal. Chem.* **2006**, *78*, 4925−4930.
(8) Wlodkowic, D.; Faley, S.; Zagnoni, M.; Wikswo, J. P.; Cooper, J. M. *Anal. Chem.* **2009**, *81*, 5517−5523.
(9) Figueroa, X. A.; Cooksey, G. A.; Votaw, S. V.; Horowitz, L. F.; Folch, A. *Lab Chip* **2010**, *10*, 1120−1127.
(10) Hosokawa, M.; Hayashi, T.; Mori, T.; Yoshino, T.; Nakasono, S.; Matsunaga, T. *Anal. Chem.* **2011**, *83*, 3648−3654.
(11) Behrens, M.; Born, S.; Redel, U.; Voigt, N.; Schuh, V.; Raguse, J.-D.; Meyerhof, W. *PLoS One* **2012**, *7*, e40304.
(12) Fitzpatrick, E.; Mcbride, S.; Yavelow, J.; Najmi, S.; Zanzucchi, P.; Wieder, R. *Clin. Chem.* **2006**, *52*, 1080−1088.
(13) Falsey, J. R.; Renil, M.; Park, S.; Li, S.; Lam, K. S. *Bioconjugate Chem.* **2001**, *12*, 346−353.
(14) Venkatesan, C.; Chrzaszcz, M.; Choi, N.; Wainwright, M. S. *J. Neuroinflammation* **2010**, *7*, 32.
(15) Green, J. V.; Sun, D.; Hafezi-Moghadam, A.; Lashkari, K.; Murthy, S. K. *Biomed. Microdevices* **2011**, *13*, 573−583.
(16) Marangoni, A.; Sambri, V.; Storni, E.; D'Antuono, A.; Negosanti, M.; Cevenini, R. *Clin. Diagn. Lab. Immunol.* **2000**, *7*, 417−421.
(17) Anagnostou, V. K.; Dimou, A. T.; Botsis, T.; Killiam, E. J.; Gustavson, M. D.; Homer, R. J.; Boffa, D.; Zolota, V.; Dougenis, D.; Tanoue, L.; Gettinger, S. N.; Detterbeck, F. C.; Syrigos, K. N.; Bepler, G.; Rimm, D. L. *Cancer* **2012**, *118*, 1607−1618.
(18) Lizzi, A. R.; D'Alessandro, A. M.; Bozzi, A.; Cinque, B.; Oratore, A.; D'Andrea, G. *Mol. Cell. Biochem.* **2007**, *300*, 29−37.
(19) Branco, L. M.; Garry, R. F. *Virol. J.* **2009**, *6*, 147.
(20) Ohtsubo, K.; Marth, J. D. *Cell* **2006**, *126*, 855−867.
(21) Varki, A. *Nature* **2007**, *446*, 1023−1029.
(22) Arndt, N. X.; Tiralongo, J.; Madge, P. D.; von Itzstein, M.; Day, C. J. *J. Cell. Biochem.* **2011**, *112*, 2230−2240.
(23) Tao, S. C.; Li, Y.; Zhou, J.; Qian, J.; Schnaar, R. L.; Zhang, Y.; Goldstein, I. J.; Zhu, H.; Schneck, J. P. *Glycobiology* **2008**, *18*, 761−769.
(24) Yamada, K.; Hyodo, S.; Kinoshita, M.; Hayakawa, T.; Kakehi, K. *Anal. Chem.* **2010**, *82*, 7436−7443.
(25) Klapoetke, S.; Zhang, J.; Becht, S.; Gu, X.; Ding, X. *J. Pharm. Biomed. Anal.* **2010**, *53*, 315−324.
(26) Gustafsson, A.; Sjoblom, M.; Strindelius, L.; Johansson, T.; Fleckenstein, T.; Chatzissavidou, N.; Lindberg, L.; Ångstrom, J.; Rova, U.; Holgersson, J. *Glycobiology* **2011**, *21*, 1071−1086.
(27) Han, E.; Ding, L.; Ju, H. *Anal. Chem.* **2011**, *83*, 7006−7012.
(28) Zhao, W. W.; Zhang, L.; Xu, J. J.; Chen, H. Y. *Chem. Commun.* **2012**, *48*, 9456−9458.
(29) Cao, J. T.; Hao, X. Y.; Zhu, Y. D.; Sun, K.; Zhu, J. J. *Anal. Chem.* **2012**, *84*, 6775−6782.
(30) Chen, S.; Zheng, T.; Shortreed, M. R.; Alexander, C.; Smith, L. M. *Anal. Chem.* **2007**, *79*, 5698−5702.
(31) Ding, L.; Cheng, W.; Wang, X.; Ding, S.; Ju, H. *J. Am. Chem. Soc.* **2008**, *130*, 7224−7225.
(32) Zan, F.; Dong, C. Q.; Liu, H.; Ren, J. C. *J. Phys. Chem. C* **2012**, *116*, 3944−3950.
(33) Gao, X.; Wu, J.; Wei, X.; He, C.; Wang, X.; Guo, G.; Pu, Q. *J. Mater. Chem.* **2012**, *22*, 6367−6373.
(34) Li, J.; Zhong, X.; Cheng, F.; Zhang, J. R.; Jiang, L. P.; Zhu, J. J. *Anal. Chem.* **2012**, *84*, 4140−4146.
(35) Peng, J.; Gao, W.; Gupta, B. K.; Liu, Z.; Romero-Aburto, R.; Ge, L.; Song, L.; Alemany, L. B.; Zhan, X.; Gao, G.; Vithayathil, S. A.; Kaipparettu, B. A.; Marti, A. A.; Hayashi, T.; Zhu, J. J.; Ajayan, P. M. *Nano Lett.* **2012**, *12*, 844−849.
(36) Park, J.; Nam, J.; Won, N.; Jin, H.; Jung, S.; Jung, S.; Cho, S.-H.; Kim, S. *Adv. Funct. Mater.* **2011**, *21*, 1558−1566.
(37) Zhelev, Z.; Ohba, H.; Bakalova, R.; Jose, R.; Fukuoka, S.; Nagase, T.; Ishikawa, M.; Baba, Y. *Chem. Commun.* **2005**, 1980−1982.
(38) Liu, A.; Peng, S.; Soo, J. C.; Kuang, M.; Chen, P.; Duan, H. *Anal. Chem.* **2011**, *83*, 1124−1130.
(39) Chen, C.; Peng, J.; Xia, H. S.; Yang, G. F.; Wu, Q. S.; Chen, L. D.; Zeng, L. B.; Zhang, Z. L.; Pang, D. W.; Li, Y. *Biomaterials* **2009**, *30*, 2912−2918.
(40) Zhao, L.; Cheng, P.; Li, J.; Zhang, Y.; Gu, M.; Liu, J.; Zhang, J.; Zhu, J. J. *Anal. Chem.* **2009**, *81*, 7075−7080.
(41) Xia, Y.; Whitesides, G. M. *Angew. Chem., Int. Ed.* **1998**, *37*, 550−575.
(42) Rettig, J. R.; Folch, A. *Anal. Chem.* **2005**, *77*, 5628−5634.
(43) Park, S.; Kim, W.; Kim, Y.; Son, Y. D.; Lee, S. C.; Kim, E.; Kim, S. H.; Kim, J. H.; Kim, H. S. *Anal. Chem.* **2010**, *82*, 5830−5837.
(44) Yin, H.; Zhang, X.; Pattrick, N.; Klauke, N.; Cordingley, H. C.; Haswell, S. J.; Cooper, J. M. *Anal. Chem.* **2007**, *79*, 7139−7144.
(45) Lis, H.; Sharon, N. *Chem. Rev.* **1998**, *98*, 637−674.
(46) Fuster, M. M.; Esko, J. D. *Nat. Rev. Cancer* **2005**, *5*, 526−542.
(47) Thomas, C. L.; Maule, A. J. *J. Gen. Virol.* **2000**, *81*, 1851−1855.
(48) Pelicano, H.; Martin, D.; Xu, R.-H.; Huang, P. *Oncogene* **2006**, *25*, 4633−4646.
(49) Hersey, P.; Watts, R. N.; Zhang, X. D.; Hackett, J. *Clin. Cancer Res.* **2009**, *15*, 6490−6494.
(50) Zhang, X. D.; Deslandes, E.; Villedieu, M.; Poulain, L.; Duval, M.; Gauduchon, P.; Schwartz, L.; Icard, P. *Anticancer Res.* **2006**, *26*, 3561−3566.
(51) Kurtoglu, M.; Gao, N.; Shang, J.; Maher, J. C.; Lehrman, M. A.; Wangpaichitr, M.; Savaraj, N.; Lane, A. N.; Lampidis, T. J. *Mol. Cancer Ther.* **2007**, *6*, 3049−3058.
(52) Elbein, A. D. *Annu. Rev. Biochem.* **1987**, *56*, 497−534.
(53) Kurtoglu, M.; Maher, J. C.; Lampidis, T. J. *Antioxid. Redox. Sign.* **2007**, *9*, 1383−1390.
(54) Andresen, L.; Skovbakke, S. L.; Persson, G.; Hagemann-Jensen, M.; Hansen, K. A.; Jensen, H.; Skov, S. *J. Immunol.* **2012**, *188*, 1847−1855.
(55) Helenius, A.; Aebi, M. *Science* **2001**, *291*, 2364−2369.